

Water Resources Research

RESEARCH ARTICLE

10.1002/2017WR020428

The effect of sampling effort on estimates of methane ebullition from peat

Jorge A. Ramirez^{1,2} , Andy J. Baird¹ , and Tom J. Coulthard³
¹School of Geography, University of Leeds, Leeds, UK, ²University of Bern, Institute of Geography, Bern, Switzerland,

³School of Environmental Sciences, University of Hull, Hull, UK

Key Points:

- Modeled ebullition and gas storage replicate patterns in natural peats
- Peat structure contributes directly to the variability of ebullition in space and time
- Traditional methods to measure ebullition can equally overestimate and underestimate flux by 20%

Supporting Information:

- Supporting Information S1

Correspondence to:

J. A. Ramirez,
jorge.ramirez@giub.unibe.ch

Citation:

Ramirez, J. A., A. J. Baird, and T. J. Coulthard (2017), The effect of sampling effort on estimates of methane ebullition from peat, *Water Resour. Res.*, 53, 4158–4168, doi:10.1002/2017WR020428.

Received 17 JAN 2017

Accepted 1 MAY 2017

Accepted article online 8 MAY 2017

Published online 22 MAY 2017

Abstract We investigated the effect of sample size and sampling duration on methane bubble flux (ebullition) estimates from peat using a computer model. A field scale (10 m), seasonal (>100 days) simulation of ebullition from a two-dimensional (2-D) structurally varying peat profile was modeled at fine spatial resolution (1 mm × 1 mm). The spatial and temporal scale of this simulation was possible because of the computational efficiency of the reduced-complexity approach that was implemented, and patterns of simulated ebullition were consistent with those found in the field and laboratory. The simulated ebullition from the peat profile suggested that decreases in peat porosity—which cause increases in gas storage—produce ebullition that becomes increasingly patchy in space and erratic in time. By applying different amounts of spatial and temporal sampling effort, it was possible to determine the uncertainty in ebullition estimates from the peatland. The results suggest that traditional methods to measure ebullition can equally overestimate and underestimate flux by 20% and large ebullition events can lead to large overestimations of flux when sampling effort is low. Our findings support those of field studies, and we recommend that ebullition should be measured frequently (hourly to daily) and at many locations ($n > 14$).

1. Introduction

Methane (CH₄) is a greenhouse gas with a global warming potential much greater than carbon dioxide [Myhre *et al.*, 2013], and one of the major sources of naturally occurring CH₄ is peatlands [Blodau, 2002; Lai, 2009]. Large amounts of CH₄ can be transported from peat to the atmosphere via diffusion through the soil, via plant-mediated transport, and as bubbles (ebullition) [Baird *et al.*, 2004; Glaser *et al.*, 2004; Chanton, 2005; Stamp *et al.*, 2013]. The last of these processes—ebullition—can show considerable spatial and temporal variability [Christensen *et al.*, 2003; Tokida *et al.*, 2007; Stamp *et al.*, 2013] which can present challenges when attempting to establish the strength of CH₄ sources in different types of peatlands. Over a few meters, peatlands can display pronounced spatial variability in vegetation composition [Bubier *et al.*, 1995; Pelletier *et al.*, 2007], the position of the water table [Bubier *et al.*, 1993; Laine *et al.*, 2007; Bon *et al.*, 2014; Chen and Slater, 2015], near-surface peat temperature [Bubier *et al.*, 1995], microtopography [Belyea and Clymo, 2001] rates of decomposition and peat properties more generally [Belyea, 1996; Moore *et al.*, 2007; Baird *et al.*, 2016]. Each of these factors may have an effect on where and when ebullition occurs, and the spatial variability of ebullition may partly reflect the spatial patterns of these factors. For example, it has been suggested that variability in peat structure, including porosity, imparts a strong influence on ebullition [Comas *et al.*, 2008; Ramirez *et al.*, 2016]. Differences in peatland permeability have also been advanced as an explanation for ebullition hotspots as well as for locations where ebullition occurs rarely or not at all. For example, in a study measuring changes in bog elevation, Glaser *et al.* [2004] recorded rapid decreases in bog elevation caused apparently by the escape of bubbles that had built up below layers of low-permeability woody peat that had ruptured (because of the buoyancy of the bubble mass). Strack *et al.* [2006] measured ebullition at two sites located within a fen and suggested that peat structural differences were important, as at one site with highly permeable peat ebullition occurred regularly, while in a second site that contained less permeable peat bubbles were prevented from reaching the water table.

The magnitude and frequency of ebullition are also dependent on temporal variability in environmental forcings that may drive the process. For example, short term (hourly) rising and falling atmospheric pressure can trigger large episodic ebullition events [Glaser *et al.*, 2004; Tokida *et al.*, 2007, 2009; Comas *et al.*, 2011;

Klapstein *et al.*, 2014], with Tokida *et al.* [2007] showing ebullition events coinciding with drops in atmospheric pressure—that in total comprised 50% of the total CH₄ flux from a peatland. As well as short-lived changes in atmospheric pressure, longer-term (days to weeks) variations in water-table elevation may also influence ebullition [Shurpali *et al.*, 1993; Glaser *et al.*, 2004].

Any sampling design for a field investigation of ebullition from peatlands should take into account the aforementioned factors because they will have some control on where ebullition occurs in a study area and whether the ebullition is characteristically erratic, or occurs regularly. If ebullition is spatially very variable, many measurement locations are needed to capture the range in flux and the site-wide average across a peatland. A study by Stamp *et al.* [2013] highlighted this point by demonstrating the amount of error in ebullition estimates when few measurement locations ($n \leq 5$) are used. In their study, seasonal ebullition from a bog was measured over two microform types (mixed sedge and *Sphagnum* lawns, and mud-bottomed hollows) using 14 inverted funnels per microform type. Overall flux varied strongly spatially, with nine funnels from the total of 28 accounting for ~76% of the summed flux, and two funnels accounting for ~30% of the total. By calculating the mean flux (per microform type) for every combination of five funnels, it was possible to estimate that there was a ~20% probability of obtaining a mean flux that was 50% less than the mean calculated with 14 funnels. This suggested that greater sampling effort ($n \gg 5$) would be necessary to obtain an accurate estimate of ebullition from a peatland with this amount of spatial variability in the process.

Similar considerations apply when ebullition is temporally very variable. Episodic or erratic ebullition may be defined by an ebullition time series that comprises mostly zero or low fluxes punctuated by infrequent, large, short-lived ebullition events. In contrast, regularly occurring or steady ebullition does not contain these large ebullition events and would not require frequent measurements to correctly estimate flux [Green and Baird, 2011]. This difference in the amount of temporal sampling effort required to measure ebullition was noted by Coulthard *et al.* [2009]. To make their point, they assumed a hypothetical ebullition series in which ebullition events were random in time and occurred on average once a day. From this assumed series they calculated that regular weekly measurements for 30 min, a sampling effort that is typical for CH₄ flux studies using manual flux chambers, would result in a 1.3% probability of recording an ebullition event. This suggests that a substantially greater number of measurements are needed to record erratic ebullition events, although the intensity required of any sampling effort will depend on the exact nature of any episodic or erratic ebullition series.

Unresolved questions from two sources—spatial and temporal sampling frequency—need to be addressed to further improve the accuracy of CH₄ ebullition estimates. Herein we focus on peatland ebullition estimates derived using static chambers. This method involves placing an air-tight enclosure over an area of peat and measuring the change in concentration of CH₄ over a short period of time (e.g., 30 min) [Tokida *et al.*, 2007]. Changes in the CH₄ concentration in the chamber can be used to estimate episodic ebullition. For example, sudden, stepped increases in CH₄ concentration are characteristic of sudden bubble releases. The degree to which episodic ebullition is captured using chambers will depend on how many are deployed and how often they are used. Given the operational difficulties of working in the field, many spatial and temporal sampling frequency questions are difficult, if not impossible, to answer via field-based experiments. Whereas in the field ebullition can only be estimated, within a model the “real” gas flux is known and it is possible to assess how well different sampling designs estimate ebullition. Therefore, we used a computer model to simulate the effect of peat structure on ebullition, and from these simulations determined what level of spatial coverage and temporal resolution is appropriate to sufficiently capture the dynamics of peatland ebullition. For this investigation, the Model of Ebullition and Gas storAge (MEGA) [Ramirez *et al.*, 2015a,b] was chosen because it is a reduced-complexity model that can be used to simulate relatively large spatial domains (unlike, for example, more detailed computational fluid dynamics models). MEGA captures the essential nature of ebullition in peat soils through its representation of key processes like the movement, storage, and release of gas from a peat pore structure (see supporting information for more details about MEGA). Our aim was to answer the following research questions: (i) How many sites are required to estimate ebullition flux from a variably structured peatland with an acceptable degree of confidence? (ii) What is the effect of ebullition flux measurement duration on the certainty of ebullition estimates? Although we focused on the measurement effort required to estimate ebullition losses from peats, and how this is affected by soil properties such as permeability, our work is also of relevance to

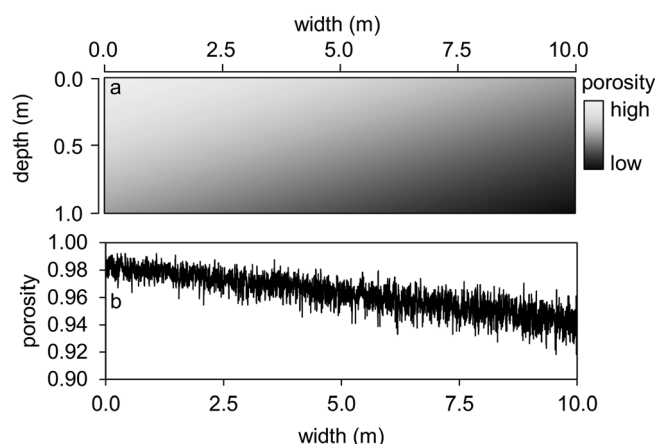


Figure 1. (a) Representation of porosity in spatially variable peat profile. (b) Porosity of profile calculated vertically (at each horizontal position the porosity for a vertical stack of cells was calculated).

understanding the build-up and loss of gasses from quasi-saturated soils [sensu Faybishenko, 1995], which in turn will affect rates of water flow below the water table [e.g., Beckwith and Baird, 2001].

2. Methods

In MEGA ebullition from a field-scale 2-D (10 m long and 1 m deep) profile of spatially heterogeneous peat was simulated. The grid cell size was set to 1 mm \times 1 mm (Figure 1a), and this resulted in a profile partitioned into 10,000,000 cells, with 1000 rows and 10,000 columns. A 10 m profile was chosen because it covers the distance

typically required to traverse the main peat types (found under different microhabitats) in many northern peatlands [Belyea and Clymo, 2001]. The lengths of “shelves” (average shelf length = 5.7 mm, standard deviation = 0.8 mm), which in MEGA represent the peat matrix [Ramirez et al., 2015a, 2015b], were set according to measurements of *Sphagnum* branches imaged using x-ray tomography [Kettridge and Binley, 2008]. Shelf placement throughout the profile was determined using two right trapezoidal distributions, with one of the distributions used to randomly select a row within the profile and the second distribution to randomly select a column. Using this method it was possible to produce a variable peat structure that changed in porosity along a vertical and horizontal gradient (Figure 1a). In general, the peat profile had higher porosity shelf arrangements near the peat surface and toward the left side of the profile. Although natural peat was not used directly to guide the placement of shelves, higher porosity shelf arrangements represented less decomposed peat, while shelves located in deeper parts of the profile represented peat undergoing compression and more advanced decomposition [Boelter, 1965; Quinton et al., 2000, 2008]. The resulting profile had porosities (Figure 1b) that were similar to measured values of porosity (91–98%) in shallow northern [Beckwith and Baird, 2001; Warner et al., 2007; Kettridge and Binley, 2008, 2011; Parsekian et al., 2012] and subtropical [Wright and Comas, 2016] peatlands.

The rate of bubble production across the peat profile was based on data from Stamp et al. [2013], who reported maximum, seasonally averaged, bubble fluxes of 709 mL $\text{m}^{-2} \text{d}^{-1}$ from mixed sedge and *Sphagnum* lawns in a Welsh raised bog. Assuming a CH_4 concentration of 5% [Tokida et al., 2005; Stamp et al., 2013], this bubble flux is equivalent to 0.025 g $\text{CH}_4 \text{m}^{-2} \text{d}^{-1}$ and is within range of CH_4 production values for northern systems (0–5 g $\text{CH}_4 \text{m}^{-2} \text{d}^{-1}$) [Sundh et al., 1994; Le Mer and Roger, 2001; Comas et al., 2008]. The smallest bubble within MEGA was 1 mm² in area and the up-scaled flux for the 10 m, 2-D profile resulted in 7090 mm² bubbles d^{-1} available to construct an hourly CH_4 production signal (bubbles h^{-1}) based on the diurnal patterns observed by Panikov et al. [2007]. To reflect the spatial variability in CH_4 production at different depths [Sundh et al., 1994; Frenzel and Karofeld, 2000; Strack and Waddington, 2008], this production signal was composed of three subsignals added randomly to the modeled peat profile at three depth zones (0.0–0.3, 0.3–0.6, and 0.6–1.0 m) such that the long-term average over the entire domain was 7090 bubbles d^{-1} (Figure 2). No horizontal spatial variability in CH_4 production was modeled, whereas in real peatlands it is very likely that there is such variability. Median bubble sizes from a preliminary simulation and theoretical relationships between bubble size and rise velocity within a porous medium [Corapcioglu et al., 2004] were used to set bubble velocities at a constant 1 mm s^{-1} (see supporting information for more details about bubble rise velocities).

Hourly ebullition totals were collected from every millimeter (1 cell) at the model's peat surface, which was also the height of the water table. The sizes of the individual bubbles comprising the ebullition were also recorded, as was the amount of gas stored within the profile at the end of the simulation. To establish initial

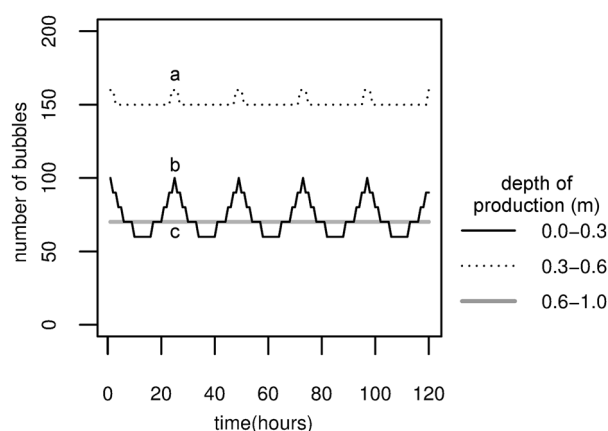


Figure 2. Methane bubble production decomposed into subsignals that are (a) weakly diurnal, (b) strongly diurnal, and (c) steady. Subsignals a, b, and c consisted of 50%, 25%, and 25% of the daily methane production accordingly and the gas equivalent in bubbles was added at three depth zones across the entire peat profile.

conditions and saturate the profile with gas, the profile was driven with the production signal until the ebullition flux, averaged over a 10 day period, stabilized. Model data collected after this time period were analyzed. The collection period was 6087 h (~254 days), and was similar in duration to a field survey measuring ebullition from peat by Goodrich *et al.* [2011]. The MEGA simulation took 222 h to complete on a single computer with a six core processor on 12 threads operating in parallel.

Bootstrapping is a method to gauge the accuracy of observations and determine how many sampling points may be appropriate [Stamp *et al.*, 2013]. In summary, bootstrapping begins by randomly selecting (with replacement) a sample of n records from the available observations (e.g., ebullition fluxes), and calculating a sample statistic (e.g., average hourly ebullition) [Efron, 1979; Sokal and Rohlf, 1995].

This process of randomly selecting records, and calculating a sample statistic is repeated many times (100–1000 s of replicates) to obtain a distribution of sample statistics. Afterward, the precision of the sample statistics, given a certain amount of sampling effort (n), can be gauged by calculating the sample statistic's standard deviation or confidence intervals. Herein, bootstrapping was performed on ebullition from the modeled peatland that was spatially variable in structure. It would have been preferable to bootstrap field observations of ebullition from structurally different peats, but this was unfeasible given the number of sampling sites ($n = 20$ —see below) and frequency of measurements (hourly) required. Thus bootstrapping the ebullition from the computer model provided a general indication of the errors involved in field sampling peatlands, and this method could show if researchers are falling short of the sampling effort needed for reliable estimates of site-wide ebullition.

As noted above, it was assumed that the ebullition would be sampled using static chambers that were placed on the peat surface. Rates of ebullition in MEGA were calculated as total ebullition (bubbles), per hour, per chamber. This was accomplished by subdividing the peat profile into 40 subprofiles, with each subprofile capable of being monitored by a chamber having a width of 250 mm. These chambers were placed end to end on the modeled peat surface and, from these 40 chambers, random combinations of chambers were created for bootstrapping.

Temporal sampling effort was determined by the time interval (e.g., hourly, daily, weekly) at which a chamber was placed on the peat surface. For each placement, 1 h of ebullition was recorded. Temporal sampling effort at long time intervals (e.g., 168 h) were chosen to represent traditional chamber methods that sample sites infrequently (weekly) [Coulthard *et al.*, 2009], and shorter time intervals (e.g., 1 h) represented frequent sampling using automated chambers [Goodrich *et al.*, 2011]. A total of 580 combinations of chambers and sampling time intervals were considered. This included between 1 and 20 chambers and sampling time intervals between 1 and 168 h, incrementing by 6 h. Average ebullition was calculated from each combination of chamber and sampling time interval and this was repeated 1000 times to create a distribution of average ebullition. To gauge the uncertainty of the average ebullition, the 95% confidence interval of each distribution was then calculated (see supporting information for more details about bootstrapping).

To quantify the effect of different amounts of sampling effort (spatial and temporal), the relative error between the average of the ebullition distributions and the true average ebullition were calculated. Furthermore, the error between the 95% confidence interval (lower and upper) of the ebullition distributions and the true average ebullition were calculated. All relative errors are presented as percentages.

3. Results

During the 254 model days, the mean individual bubble size was 4 mm^2 , with a minimum and maximum individual bubble size of 1 and 115 mm^2 , respectively. Overall bubble sizes from the peat profile display a power law pattern (Figure 3a), with many occurrences of small bubbles and fewer large bubbles. For every hour of the 6087 h simulation, at least one ebullition event, consisting of multiple bubbles, occurred somewhere across the model domain (i.e., the entire peat profile). The smallest hourly ebullition event was 79 bubbles and the largest 609 bubbles. The mean hourly ebullition was 299 bubbles. Plotting the magnitude and frequency of ebullition events (Figure 3b) produces a histogram that is nonnormal and positively skewed (skewness = 0.5; $n = 6087$; this value was interpreted as moderate skewness). Skewness was calculated with a formula adjusting for the sample size [Joanes and Gill, 1998].

Gas storage at the end of the simulation was 11% of the overall model domain, but structural differences within the peat profile led to spatial variability in gas storage. This variability in gas storage was a result of the two gradients (horizontal and vertical) that were used to position the “shelves” representing the peat matrix within the profile. Across the profile, from left to right, the porosity of the shelf arrangements, when measured vertically per mm width (along the x axis), decreased from 98% to 93% and gas storage, measured in the same manner, increased linearly from 3% to 37% (Figure 4a). This positive trend in gas storage can also be visualized in three subsets of the profile taken at the end of the simulation (Figure 4b). By calculating the peat porosity and bubble storage of each subset, it was possible to ascertain that the subset from the left side of the profile (Figure 4b, inset 1) had a peat porosity that is high (98%) and a low amount of gas storage (5%). In contrast the subset from the right side of the profile (Figure 4b, inset 3) had lower peat porosity (95%), and higher gas storage (23%). At the bottom-right of Figure 4b plot 3, the local porosity over a $200 \text{ mm} \times 200 \text{ mm}$ area is the lowest for the entire profile (92%). This represents the lower end of porosity values for northern peatlands and produces locally high gas contents (62%). These accumulations are representative of gas content underneath well-decomposed layers of peat or semipermeable layers that obstruct the upward movement of gas [Rosenberry *et al.*, 2003; Glaser *et al.*, 2004].

The effect of the vertical gradient used to place more shelves at greater depths contributed to more bubble storage at the base of the peat profile. Thirty-two percent of the bubbles stored in the entire profile were located at depths $\leq 0.5 \text{ m}$, with 68% at deeper locations ($>0.5 \text{ m}$). This difference in bubble storage is most evident on the right side of the profile (Figure 4b, inset 3) where gas storage was greatest at a depth near 1 m.

Of the 10 m of peat simulated, only 47% of the peat surface emitted ebullition, and 50% of the ebullition came from 3% of the profile. Overall the ebullition from the profile became more variable in space with lower peat porosities (as controlled by shelf density). The effect of peat porosity on the location of ebullition can be seen by comparing the higher porosity, left side of the profile (LSP, distance across the profile from 0 to 5 m) with the lower porosity, right side of the profile (RSP, distance across the profile from 5 to 10 m). Although both sides of the profile produced similar amounts of ebullition ($\sim 900,000$ bubbles), the RSP had greater spatial variability with highly irregular ebullition, and the LSP produced ebullition more uniformly in

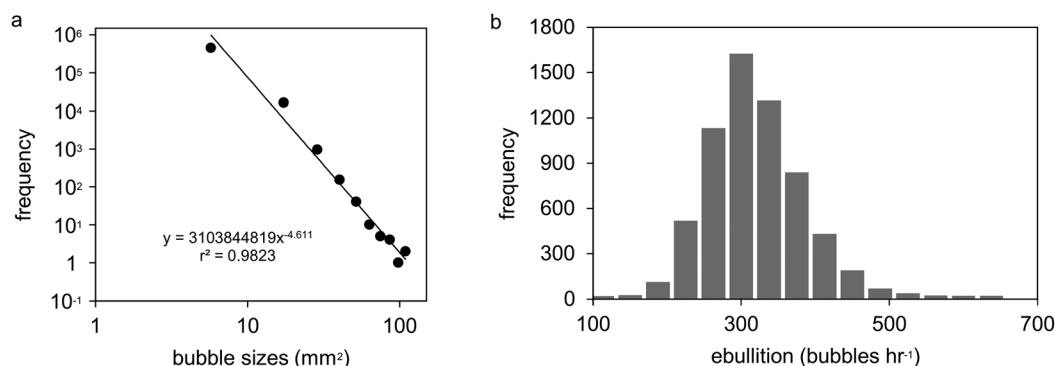


Figure 3. (a) Magnitude and frequency of bubble size from profile with fitted power law distribution ($p < 0.05$). (b) Magnitude and frequency of hourly ebullition from profile.

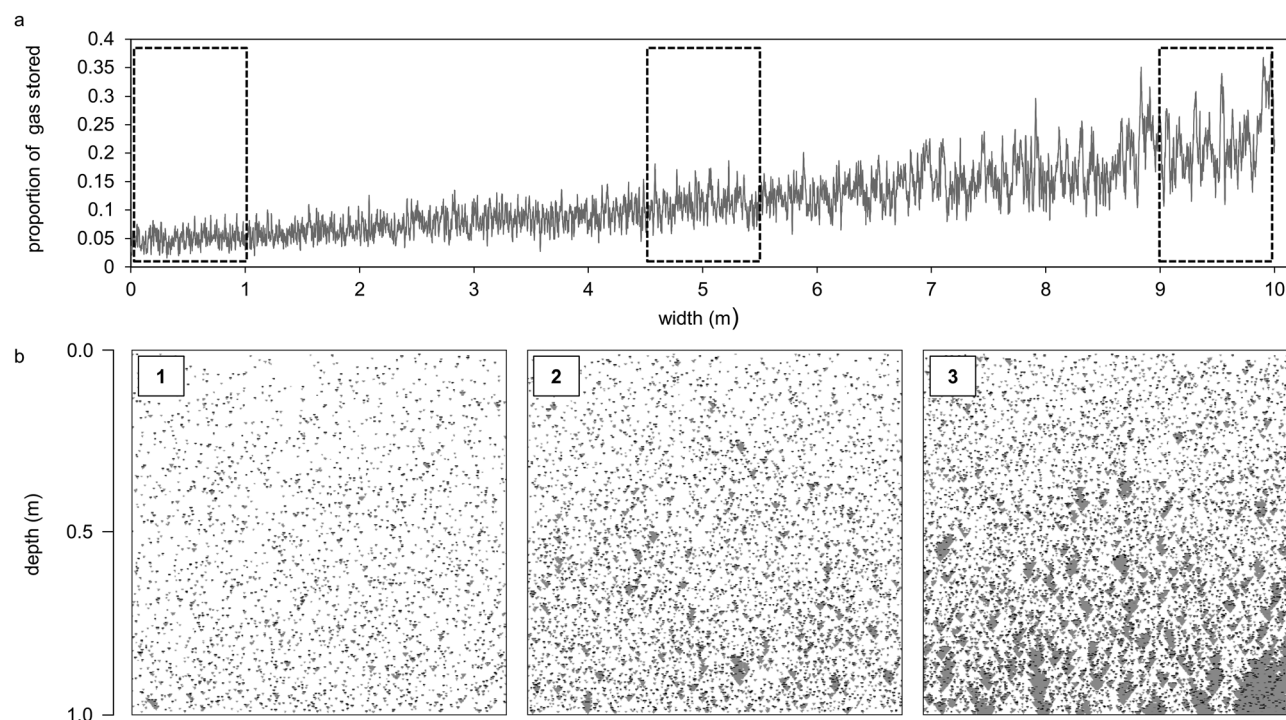


Figure 4. (a) Proportion of vertical gas storage per millimeter of peat profile. Dashed boxes correspond to shelf arrangements below. (b) Examples of gas storage for (1) high, (2) moderate, and (3) low porosity shelf arrangements (peat fibres/particles in black, gas in grey, and water in white).

space (Figure 5). Locations of extreme ebullition were identified using the 99.9th percentile of the total ebullition across the profile. Using this cut-off, locations of greater ebullition only occurred on the RSP (Figure 5, dashed line = 99.9th percentile). Furthermore, these extreme amounts of ebullition were proximate to locations of low ebullition and this disparity in ebullition contributed to greater spatial variability in ebullition from the RSP.

The temporal variability of hourly ebullition was also dependent on the porosity of the underlying shelf arrangements. Over the course of the 254 simulated days, the high porosity LSP and low porosity RSP had noticeably different amounts of temporal variability in ebullition (Figures 6a and 6b). Both sides of the profile had similar mean hourly ebullition (~ 150 bubbles h^{-1}), but the RSP generated hourly ebullition that was more erratic (min = 15 bubbles h^{-1} , max = 498 bubbles h^{-1} , st. dev. = 46 bubbles h^{-1}) than ebullition from the LSP (min = 46 bubbles h^{-1} , max = 337 bubbles h^{-1} , st. dev. = 37 bubbles h^{-1}). Moreover, the extremely large hourly ebullition events (>99.9 th percentile) only occurred on the RSP (Figures 6a and 6b, dashed line = 99.9th percentile). The erratic nature of ebullition from the RSP can also be identified in side-by-side histograms of hourly ebullition from the LSP and RSP (Figure 6c). The RSP produced considerably more small (<100 bubbles) and large (>350 bubbles) ebullition events than the LSP.

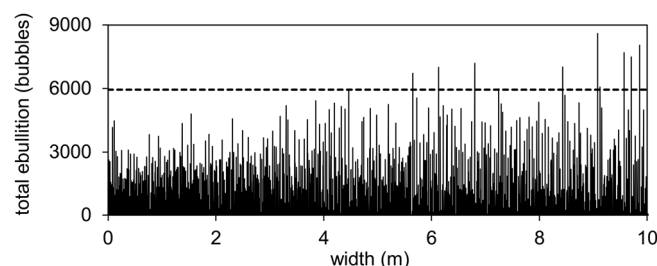


Figure 5. Total ebullition from peat profile, black dashed line is 99.9th percentile of total ebullition.

The true average ebullition from the modeled peat profile was 7.5 bubbles $\text{chamber}^{-1} \text{h}^{-1}$. Error in average ebullition estimates decreases with greater spatial and temporal sampling effort. This trend is visible in the decreasing amount of error in the averages and 95% confidence intervals of ebullition distributions produced by performing the bootstrapping resampling with 1–20 chambers, and visiting the profile once every hour, day, or week (Figure 7a).

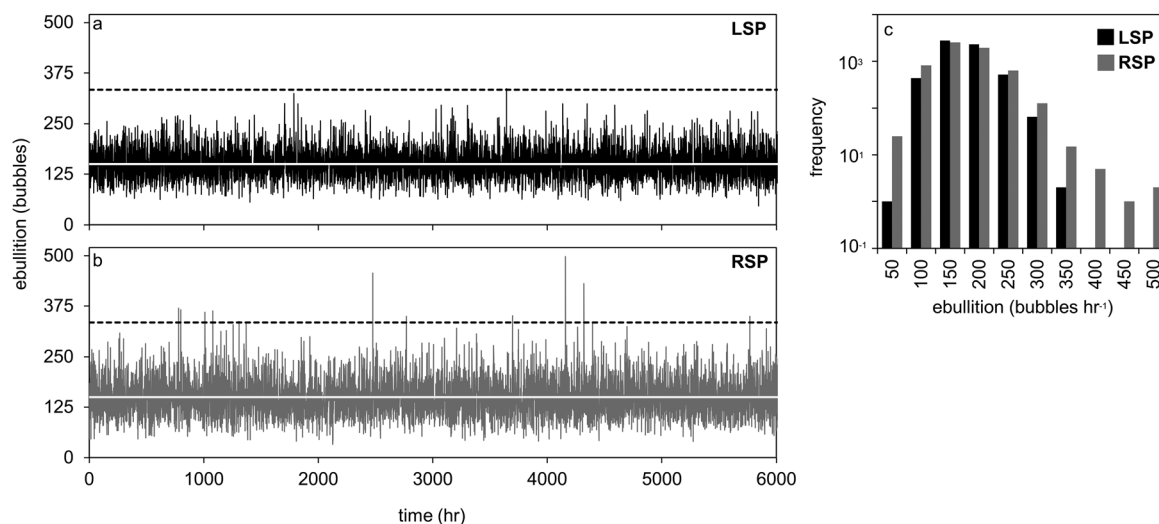


Figure 6. Hourly ebullition events from the (a) left side of the profile (LSP) and (b) right side of the profile (RSP). Dashed line is 99.9th percentile of hourly ebullition events from the entire profile and white line is the mean hourly ebullition (~ 150 bubbles h^{-1}). (c) Histograms of the hourly ebullition events from the LSP and RSP.

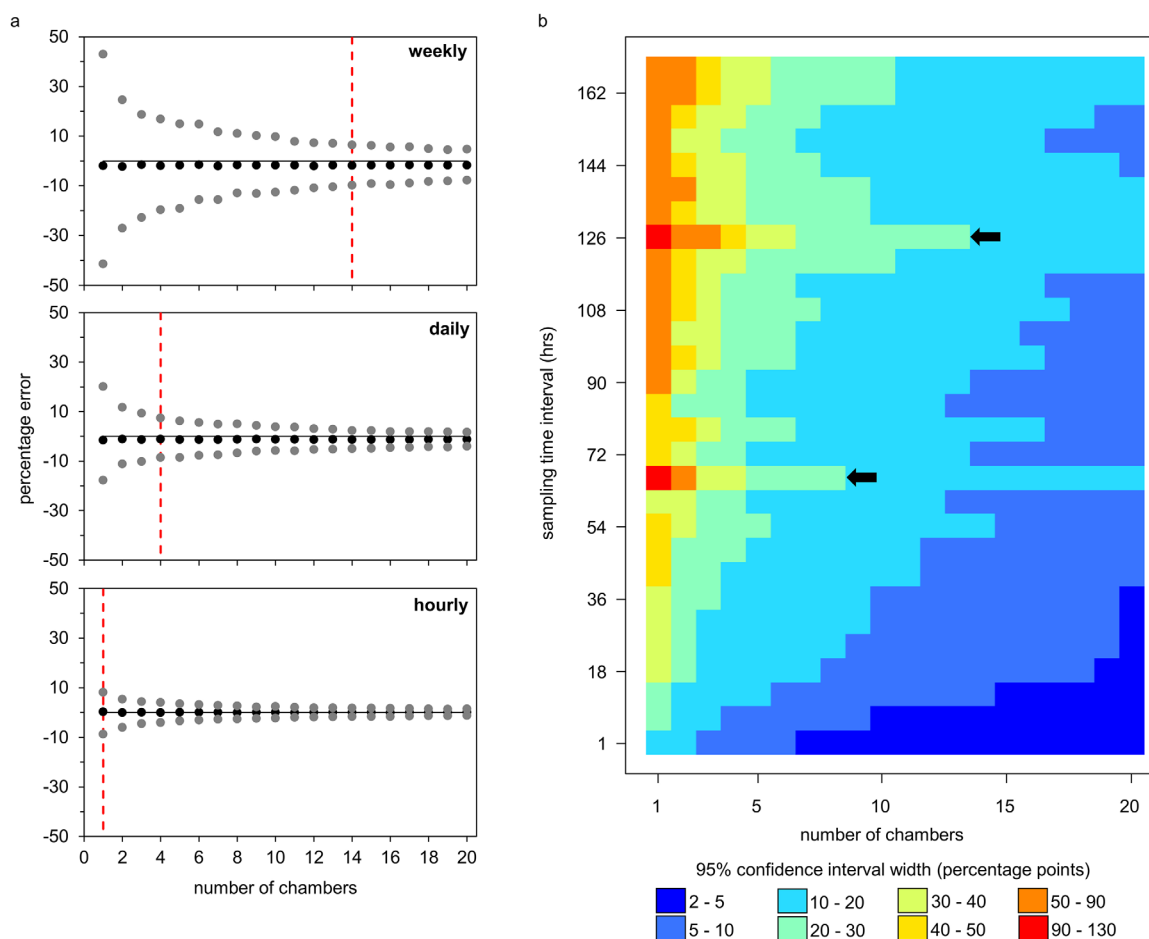


Figure 7. (a) Percentage error between the true average ebullition and the average (black points) and 95% confidence interval (grey points) of the average ebullition distributions from 1 to 20 chambers sampled weekly, daily, and hourly. Dashed red line indicates locations of $\pm 10\%$ error. (b) Error map representing the width of the 95% confidence interval of the average ebullition distributions. Black arrows indicate peaks in error.

Comparable amounts of error can be obtained with different amounts of sampling effort. For example, to obtain a maximum of $\pm 10\%$ error in average ebullition the profile could be sampled with 14 chambers every week, four chambers every day, or one chamber every hour (Figure 7a, dashed lines). These error plots (Figure 7a) also show that the upper and lower confidence intervals are nearly symmetrical, indicating an equal probability of over or under estimating average ebullition for these sampling combinations.

Another approach to visualize the error in the average ebullition is to calculate the width of the 95% confidence interval (i.e., the area between the upper and lower confidence intervals) (Figure 7b). As before, the amount of possible error in predicting the true average ebullition is provided as a relative error. Figure 7b summarizes the possible error for each combination of chamber and sampling time interval as an error map. From the error map, it is possible to distinguish regions with similar amounts of error, but different amounts of sampling effort. For example, the lower right corner of the map indicates sampling schemes that produce the lowest amount of error. This includes schemes with high temporal and low spatial sampling effort (e.g., seven chambers sampled hourly) or moderate temporal and high spatial sampling effort (e.g., 20 chambers sampled every 36 h). Unexpectedly, the greatest amount of error does not correspond to sampling with the fewest chambers, and sampling infrequently (1 chamber, every 168 h). Instead error is greatest with one chamber visited every 126 h and the second largest amount of error occurs with one chamber visited every 66 h.

4. Discussion

Ebullition from the simulated peat profile resulted in a positively skewed distribution of ebullition events and was similar in shape to results reported by researchers measuring ebullition from peat in the field [Kellner *et al.*, 2006; Goodrich *et al.*, 2011; Stamp *et al.*, 2013] and laboratory experiments [Yu *et al.*, 2014; Ramirez *et al.*, 2016]. The simulated ebullition comprised bubble sizes that displayed power law patterns, and these were consistent with patterns found from laboratory experiments on peat [Ramirez *et al.*, 2016]. Overall gas storage within the peat profile was 11% and within the range of gas storage reported in northern peatlands (see Rosenberry *et al.* [2006] for review). Modeled vertical gas storage per millimeter of peat profile was between 3% and 37%, and was comparable to gas content (0–32%) directly sampled from northern peats with porosities (96–99%) similar to the modeled peat profile (93–98%) [Strack and Mierau, 2010]. Furthermore, the spatial distribution of storage in the simulation was dependent on the porosity of the shelf arrangements. Here low-porosity shelf arrangements in the profile represent peat with small pores and form a barrier within the profile that traps large quantities of gas. In contrast, high-porosity shelf arrangements in the profile are peats with large pores and allow gas to move more freely through the profile. This open peat structure stores lower amounts of gas within the peat profile. At the base of the profile the porosity was lower and large amounts of gas accumulated underneath the shelves representing the peat. These gas trapping properties have also been observed in peats with lower porosity [Glaser *et al.*, 2004; Strack and Mierau, 2010].

The structure of the peat profile in this simulation contributed directly to the variability of ebullition in space and time. Here the variability in ebullition was directly caused by the porosity of the peat (shelf arrangements) and the resulting amounts of bubble storage, because no environmental controls, such as changes in atmospheric pressure or water-table position, were simulated. Within MEGA, high porosity shelf arrangements cannot trap large quantities of gas and the resulting bubbles are emitted steadily. However, if low-porosity shelf arrangements (e.g., woody layers or well-decomposed layers of peat) exist bubbles can accumulate and are released as pulses or bursts (i.e., cyclical or episodic releases). Here locations in the profile with high peat porosity and low bubble storage had few bubbles available for erratic or episodic ebullition. These conditions were found in the LSP and resulted in ebullition that occurred uniformly in space, and regularly in time. In contrast, low peat porosity and high bubble storage resulted in large quantities of stored bubbles. These isolated bubble storage “hotspots” were found in the RSP, and resulted in ebullition that was spatially irregular and temporally erratic.

The near vertical banding in the error map (Figure 7b) indicates that error in ebullition was more dependent on the number of chambers deployed than the frequency of measurements performed. Where the vertical banding was irregular, temporal variability in ebullition contributed to uncertainty in ebullition estimates. This uncertainty was greatest when sampling the profile at time intervals of 66 and 126 h (Figure 7b, black

arrows). At these sampling intervals, the error propagated through the error map as horizontal peaks. This pattern suggests that increasing the spatial sampling effort at these sampling intervals (66 and 126 h) has a reduced effect on minimizing error. To understand these unexpected horizontal peaks in the error map, the variability in the ebullition was examined at these sampling intervals. The temporal variability of ebullition across the entire profile at the time intervals of 66 and 126 h reveals that a large spike in ebullition was recorded in both time series (time = 4158 h). Furthermore, the spatial distribution of this ebullition spike was distributed across the peat profile in a highly clustered manner. This resulted in an ebullition “hot-spot” that occurred within one chamber (chamber 38). The overall effect of this ebullition spike concentrated over a small area of the profile contributed toward the overestimation of average ebullition. From the perspective of temporal sampling effort, the low number of records obtained when sampling the peat every 66 and 126 h, $n = 93$ and $n = 49$, respectively, allowed the spike in ebullition to skew the average ebullition. When combining these low sample sizes, with a low number of deployed chambers, the probability of overestimating or underestimating the average was compounded. For example, sampling with one chamber visited every 126 h, the error in average ebullition may be overestimated by 88% or underestimated by 42%. The effect of the ebullition spike was reduced when the peat profile was sampled with more chambers, and increasing the number of chambers to five produced symmetrical amounts of error of $\pm 20\%$. The ebullition spike that was simulated is only an example of many ebullition spikes that could occur anywhere in time and more than likely from low porosity peat if the model were to be rerun and the analysis repeated.

The variability in ebullition produced error in ebullition estimates, especially when low amounts of sampling effort were used. Furthermore, this amount of error is conservative because the variability in ebullition within the model is produced solely by the storage and release of gas from the shelf arrangements below the peat surface. Greater variability and uncertainty in ebullition would be expected from a model or system that includes: (1) variable gas production, (2) external triggers that produce large bubble releases, and (3) peat containing impermeable woody layers that trap and release large amounts of gas. These are model processes and properties that can be developed in MEGA and will be the subject of future work. Another interesting result was that low sampling effort can “capture” large bubble events that likely result in ebullition overestimates. A study that bootstrapped weekly field measurements of ebullition using 250 mm diameter glass funnels recommended a sample size (e.g., number of funnels) > 14 , and found that sample sizes ≤ 5 produced considerable error in ebullition estimates [Stamp *et al.*, 2013]. Here the bootstrapping of simulated ebullition, collected with chambers of the same dimension used by Stamp *et al.* [2013], supports this conclusion. Likewise, our modeled results suggest that weekly sampling with larger sample sizes > 14 can produce conservative amounts of error (± 4 – 10%) while smaller sample sizes < 5 result in larger amounts of error (± 20 – 43%) (Figure 7a, weekly sampling). Moreover our findings suggest that the combination of larger sample sizes ($n > 14$) and frequent visitation of chambers (hourly to daily) considerably reduces error in estimates (± 1 – 5%) (Figure 7a, hourly and daily). In addition to revealing the error associated with measuring ebullition with different intensities of sampling effort, we have shown the feasibility of using MEGA at the field scale. The model simulates spatial patterns in bubble accumulation over scales that start to become relevant to understanding the wider ecohydrological behavior of peatlands [see Comas *et al.*, 2008; Baird *et al.*, 2016], and has the potential to be coupled with groundwater models, so that the effect of trapped bubbles on water storage and flow within peat soils can be simulated.

5. Conclusions

In this investigation, a field-scale (10 m) simulation of ebullition from peat was performed using MEGA. This simulation demonstrated the computational efficiency of the reduced-complexity approach implemented within MEGA. In less than 10 days of computer time, MEGA routed 100,000 s of microgas bubbles (1 mm^2) through a model peat profile consisting of shelves that were represented by a gridded structure of 10,000,000 cells. Modeled ebullition and gas storage replicate patterns in natural peats. Within the model, peat structure contributes directly to the variability of ebullition in space and time. Our results suggest that traditional methods to measure ebullition can equally overestimate and underestimate flux by 20%.

Acknowledgments

This research was supported by a postgraduate fee waiver provided by the University of Leeds's School of Geography. Contact the corresponding author for access to the data generated within this study. We would like to thank the Editor and anonymous reviewers for their suggestions for improvement on an earlier version of this paper.

References

- Baird, A. J., C. W. Beckwith, S. Waldron, and J. M. Waddington (2004), Ebullition of methane-containing gas bubbles from near-surface Sphagnum peat, *Geophys. Res. Lett.*, *31*, L21505, doi:10.1029/2004GL021157.
- Baird, A. J., A. M. Milner, A. Blundell, G. T. Swindles, and P. J. Morris (2016), Microform-scale variations in peatland permeability and their ecohydrological implications, *J. Ecol.*, *104*(2), 531–544.
- Beckwith, C. W., and A. J. Baird (2001), Effect of biogenic gas bubbles on water flow through poorly decomposed blanket peat, *Water Resour. Res.*, *37*(3), 551–558, doi:10.1029/2000WR900303.
- Belyea, L. R. (1996), Separating the effects of litter quality and microenvironment on decomposition rates in a patterned peatland, *Oikos*, *77*(3), 529–539, doi:10.2307/3545942.
- Belyea, L. R., and R. S. Clymo (2001), Feedback control of the rate of peat formation, *Proc. R. Soc. London, Ser. B*, *268*(1473), 1315–1321.
- Blodau, C. (2002), Carbon cycling in peatlands—A review of processes and controls, *Environ. Rev.*, *10*(2), 111–134, doi:10.1139/a02-004.
- Boelter, D. H. (1965), Hydraulic conductivity of peats, *Soil Sci.*, *100*(4), 227–231.
- Bon, C. E., A. S. Reeve, L. Slater, and X. Comas (2014), Using hydrologic measurements to investigate free-phase gas ebullition in a Maine peatland, USA, *Hydrol. Earth Syst. Sci.*, *18*(3), 953–965, doi:10.5194/hess-18-953-2014.
- Bubier, J., A. Costello, T. R. Moore, N. T. Roulet, and K. Savage (1993), Microtopography and methane flux in boreal peatlands, northern Ontario, Canada, *Can. J. Bot.*, *71*(8), 1056–1063.
- Bubier, J. L., T. R. Moore, L. Bellisario, N. T. Comer, and P. M. Crill (1995), Ecological controls on methane emissions from a Northern Peatland Complex in the zone of discontinuous permafrost, Manitoba, Canada, *Global Biogeochem. Cycles*, *9*(4), 455–470, doi:10.1029/95GB02379.
- Chanton, J. P. (2005), The effect of gas transport on the isotope signature of methane in wetlands, *Org. Geochem.*, *36*(5), 753–768.
- Chen, X., and L. Slater (2015), Gas bubble transport and emissions for shallow peat from a northern peatland: The role of pressure changes and peat structure, *Water Resour. Res.*, *51*, 151–168, doi:10.1002/2014WR016268.
- Christensen, T. R., N. Panikov, M. Mastepanov, A. Joabsson, A. Stewart, M. Öquist, M. Sommerkorn, S. Reynaud, and B. Svensson (2003), Biotic controls on CO₂ and CH₄ exchange in wetlands: A closed environment study, *Biogeochemistry*, *64*(3), 337–354.
- Comas, X., L. Slater, and A. Reeve (2008), Seasonal geophysical monitoring of biogenic gases in a northern peatland: Implications for temporal and spatial variability in free phase gas production rates, *J. Geophys. Res.*, *113*, G01012, doi:10.1029/2007JG000575.
- Comas, X., L. Slater, and A. S. Reeve (2011), Atmospheric pressure drives changes in the vertical distribution of biogenic free-phase gas in a northern peatland, *J. Geophys. Res.*, *116*, G04014, doi:10.1029/2011JG001701.
- Corapcioglu, M. Y., A. Cihan, and M. Drazenovici (2004), Rise velocity of an air bubble in porous media: Theoretical studies, *Water Resour. Res.*, *40*, W04214, doi:10.1029/2003WR002618.
- Coulthard, T., A. J. Baird, J. Ramirez, and J. M. Waddington (2009), Modeling methane dynamics in peat: Future prospects, in *Northern Peatlands and Carbon Cycling*, vol. 184, edited by A. J. Baird et al., 299 pp., AGU, Washington, D. C.
- Efron, B. (1979), Bootstrap methods: Another look at the jackknife, *Ann. Stat.*, 1–26.
- Faybishenko, B. A. (1995), Hydraulic behavior of quasi-saturated soils in the presence of entrapped air: Laboratory experiments, *Water Resour. Res.*, *31*(10), 2421–2435, doi:10.1029/95WR01654.
- Frenzel, P., and E. Karofeld (2000), CH₄ emission from a hollow-ridge complex in a raised bog: The role of CH₄ production and oxidation, *Biogeochemistry*, *51*(1), 91–112, doi:10.1023/a:1006351118347.
- Glaser, P. H., J. P. Chanton, P. Morin, D. O. Rosenberry, D. I. Siegel, O. Ruud, L. I. Chasar, and A. S. Reeve (2004), Surface deformations as indicators of deep ebullition fluxes in a large northern peatland, *Global Biogeochem. Cycles*, *18*, GB1003, doi:10.1029/2003GB002069.
- Goodrich, J. P., R. K. Varner, S. Frolking, B. N. Duncan, and P. M. Crill (2011), High-frequency measurements of methane ebullition over a growing season at a temperate peatland site, *Geophys. Res. Lett.*, *38*, L07404, doi:10.1029/2011GL046915.
- Green, S. M., and A. J. Baird (2011), A mesocosm study of the role of the sedge *Eriophorum angustifolium* in the efflux of methane—including that due to episodic ebullition—from peatlands, *Plant Soil*, *351*(1–2), 207–218, doi:10.1007/s11104-011-0945-1.
- Joanes, D. N., and C. A. Gill (1998), Comparing measures of sample skewness and kurtosis, *J. R. Stat. Soc., Ser. D*, *47*(1), 183–189.
- Kellner, E., A. J. Baird, M. Oosterwoud, K. Harrison, and J. M. Waddington (2006), Effect of temperature and atmospheric pressure on methane ebullition from near-surface peats, *Geophys. Res. Lett.*, *33*, L18405, doi:10.1029/2006GL027509.
- Kettridge, N., and A. Binley (2008), X-ray computed tomography of peat soils: Measuring gas content and peat structure, *Hydrol. Processes*, *22*(25), 4827–4837, doi:10.1002/hyp.7097.
- Kettridge, N., and A. Binley (2011), Characterization of peat structure using X-ray computed tomography and its control on the ebullition of biogenic gas bubbles, *J. Geophys. Res.*, *116*, G01024, doi:10.1029/2010JG001478.
- Klapstein, S. J., M. R. Turetsky, A. D. McGuire, J. W. Harden, C. I. Czimczik, X. Xu, J. P. Chanton, and J. M. Waddington (2014), Controls on methane released through ebullition in peatlands affected by permafrost degradation, *J. Geophys. Res. Biogeosci.*, *119*, 418–431, doi:10.1002/2013JG002441.
- Lai, D. Y. F. (2009), Methane dynamics in Northern Peatlands: A review, *Pedosphere*, *19*(4), 409–421.
- Laine, A., D. Wilson, G. Kiely, and K. A. Byrne (2007), Methane flux dynamics in an Irish lowland blanket bog, *Plant Soil*, *299*(1–2), 181–193, doi:10.1007/s11104-007-9374-6.
- Le Mer, J., and P. Roger (2001), Production, oxidation, emission and consumption of methane by soils: A review, *Eur. J. Soil Biol.*, *37*(1), 25–50.
- Moore, T. R., J. L. Bubier, and L. Bledzki (2007), Litter decomposition in temperate peatland ecosystems: The effect of substrate and site, *Ecosystems*, *10*(6), 949–963.
- Myhre, G., D. Shindell, F. Bréon, W. Collins, J. Fuglestad, J. Huang, D. Koch, J. Lamarque, D. Lee, and B. Mendoza (2013), Anthropogenic and natural radiative forcing Climate Change 2013, in *The Physical Science Basis. Contribution of Working Group I to the Fifth Assessment Report of the Intergovernmental Panel on Climate Change*, edited by T. F. Stocker et al., pp. 659–740, Cambridge Univ. Press, Cambridge, New York.
- Panikov, N. S., M. A. Mastepanov, and T. R. Christensen (2007), Membrane probe array: Technique development and observation of CO₂ and CH₄ diurnal oscillations in peat profile, *Soil Biol. Biochem.*, *39*(7), 1712–1723, doi:10.1016/j.soilbio.2007.01.034.
- Parsekian, A. D., L. Slater, and D. Gimenez (2012), Application of ground-penetrating radar to measure near-saturation soil water content in peat soils, *Water Resour. Res.*, *48*, W02533, doi:10.1029/2011WR011303.
- Pelletier, L., T. R. Moore, N. T. Roulet, M. Garneau, and V. Beaulieu-Audy (2007), Methane fluxes from three peatlands in the La Grande Rivière watershed, James Bay lowland, Canada, *J. Geophys. Res.*, *112*, G01018, doi:10.1029/2006JB000216.
- Quinton, W. L., D. M. Gray, and P. Marsh (2000), Subsurface drainage from hummock-covered hillslopes in the Arctic tundra, *J. Hydrol.*, *237*(1–2), 113–125, doi:10.1016/S0022-1694(00)00304-8.

- Quinton, W. L., M. Hayashi, and S. K. Carey (2008), Peat hydraulic conductivity in cold regions and its relation to pore size and geometry, *Hydrol. Processes*, 22(15), 2829–2837, doi:10.1002/hyp.7027.
- Ramirez, J. A., A. J. Baird, T. J. Coulthard, and J. M. Waddington (2015a), Ebullition of methane from peatlands: Does peat act as a signal shredder?, *Geophys. Res. Lett.*, 42, 3371–3379, doi:10.1002/2015GL063469.
- Ramirez, J. A., A. J. Baird, T. J. Coulthard, and J. M. Waddington (2015b), Testing a simple model of gas bubble dynamics in porous media, *Water Resour. Res.*, 51, 1036–1049, doi:10.1002/2014WR015898.
- Ramirez, J. A., A. J. Baird, and T. J. Coulthard (2016), The effect of pore structure on ebullition from peat, *J. Geophys. Res. Biogeosci.*, 121, 1646–1656, doi:10.1002/2015JG003289.
- Rosenberry, D. O., P. H. Glaser, D. I. Siegel, and E. P. Weeks (2003), Use of hydraulic head to estimate volumetric gas content and ebullition flux in northern peatlands, *Water Resour. Res.*, 39(3), 1066, doi:10.1029/2002WR001377.
- Rosenberry, D. O., P. H. Glaser, and D. I. Siegel (2006), The hydrology of northern peatlands as affected by biogenic gas: Current developments and research needs, *Hydrol. Processes*, 20(17), 3601–3610, doi:10.1002/hyp.6377.
- Shurpali, N. J., S. B. Verma, R. J. Clement, and D. P. Billesbach (1993), Seasonal distribution of methane flux in a Minnesota peatland measured by eddy-correlation, *J. Geophys. Res.*, 98(D11), 20,649–20,655, doi:10.1029/93JD02181.
- Sokal, R. R., and F. J. Rohlf (1995), *Biometry*, W.H. Freeman, New York.
- Stamp, I., A. J. Baird, and C. M. Heppell (2013), The importance of ebullition as a mechanism of methane (CH₄) loss to the atmosphere in a northern peatland, *Geophys. Res. Lett.*, 40, 2087–2090, doi:10.1002/grl.50501.
- Strack, M., and T. Mierau (2010), Evaluating spatial variability of free-phase gas in peat using ground-penetrating radar and direct measurement, *J. Geophys. Res.*, 115, G02010, doi:10.1029/2009JG001045.
- Strack, M., and J. M. Waddington (2008), Spatiotemporal variability in peatland subsurface methane dynamics, *J. Geophys. Res.*, 113, G02010, doi:10.1029/2007JG000472.
- Strack, M., E. Kellner, and J. M. Waddington (2006), Effect of entrapped gas on peatland surface level fluctuations, *Hydrol. Processes*, 20(17), 3611–3622, doi:10.1002/hyp.6518.
- Sundh, I., M. Nilsson, G. Granberg, and B. H. Svensson (1994), Depth distribution of microbial production and oxidation of methane in northern boreal peatlands, *Microb. Ecol.*, 27(3), 253–265.
- Tokida, T., T. Miyazaki, M. Mizoguchi, and K. Seki (2005), In situ accumulation of methane bubbles in a natural wetland soil, *Eur. J. Soil Sci.*, 56(3), 389–396.
- Tokida, T., T. Miyazaki, M. Mizoguchi, O. Nagata, F. Takakai, A. Kagemoto, and R. Hatano (2007), Falling atmospheric pressure as a trigger for methane ebullition from peatland, *Global Biogeochem. Cycles*, 21, GB2003, doi:10.1029/2006GB002790.
- Tokida, T., T. Miyazaki, and M. Mizoguchi (2009), Physical controls on ebullition losses of methane from peatlands, in *Carbon Cycling in Northern Peatlands*, vol. 184, edited by A. J. Baird et al., pp. 219–228, AGU, Washington, D. C.
- Warner, B. G., T. Asada, and N. P. Quinn (2007), Seasonal influences on the ecology of testate amoebae (Protozoa) in a small *Sphagnum* peatland in Southern Ontario, Canada, *Microb. Ecol.*, 54(1), 91–100.
- Wright, W., and X. Comas (2016), Estimating methane gas production in peat soils of the Florida Everglades using hydrogeophysical methods, *J. Geophys. Res. Biogeosci.*, 121, 1190–1202, doi:10.1002/2015JG003246.
- Yu, Z., L. D. Slater, K. V. R. Schäfer, A. S. Reeve, and R. K. Varner (2014), Dynamics of methane ebullition from a peat monolith revealed from a dynamic flux chamber system, *J. Geophys. Res. Biogeosci.*, 119, 1789–1806, doi:10.1002/2014JG002654.